Journal of Instrumentation

Cherenkov radiation from relativistic heavy ions: interpretation in terms of diffraction

Published by IOP Publishing for Sissa Medialab

Received: *February 15, 2024*
Revised: *October 7, 2024*
Accepted: *November 11, 2024*
Published: *November 15, 2024*

The XIV International Symposium on Radiation from Relativistic Electrons in Periodic Structures merged with the VIII International Conference on Electron, Positron, Neutron and X-ray Scattering under External Influences
Tsaghkadzor, Republic of Armenia
18–22 September 2023

Cherenkov radiation from relativistic heavy ions: interpretation in terms of diffraction

O.V. Bogdanov[a,b,*] **and E.I. Rozhkova**[a]

[a]*Mathematics and Mathematical Physics Division, Tomsk Polytechnic University, Lenin Ave. 30, 634050, Tomsk, Russia*
[b]*Physics Faculty, Tomsk State University, Lenin Ave. 36, 634050, Tomsk, Russia*

E-mail: bov@tpu.ru

Abstract: We demonstrate here the relationship between the diffraction theory and the theory of optical radiation in the vicinity of the Cherenkov cone from relativistic heavy ions taking account of the slowing-down in a radiator. We draw an analogy with the Huygens-Fresnel principle and demonstrate how the Cornu spiral, known in physical optics, is useful for qualitative and quantitative analysis of the shape and width of the non-trivial angular distributions of radiation.

Keywords: Cherenkov detectors; dE/dx detectors; Timing detectors; Ion identification systems

*Corresponding author.

https://doi.org/10.1088/1748-0221/19/11/C11011

Contents

2024 JINST 19 C11011

1 Introduction

Despite almost 80 years of its history, from the discovery up to date, some fine properties of optical radiation in the vicinity of the Cherenkov cone (hereinafter Vavilov-Cherenkov radiation, VChR), e.g. the spectral and angular distributions still remain largely unstudied experimentally. This is mainly due to the strong belief that the Tamm-Frank theory [1] is quite exhaustive, since it works quite reliably in calculations of geometry and the efficiency of Cherenkov detectors in high-energy physics. In refs. [2–6] the new features of this multi-faceted phenomenon are analysed, in particular — the mixed Synchrotron-Cherenkov radiation from high-energy particles in the atmosphere and mixed Cherenkov-Bremsstrahlung from relativistic heavy ions (RHI) in a matter.

The theoretically predicted changes in spectral and angular distributions of mixed optical radiation in the case of RHI, from one side may serve for suggestions of the new types of detectors, but from the other side can influence the efficiency of existing Cherenkov RHI detectors. Thus, there is a need for precision experimental studies of this mixed type of optical radiation from RHI in a matter.

I.M. Frank was the first to note the similarity between the VChR theory and the diffraction theory. He linked the condition of coherence of VChR to the Fresnel zones, for the detailed description see the review by B.M. Bolotovsky [7]. This connection is true for the VChR emission from a charged particle being in uniform and rectilinear motion in an optically transparent radiator. In the case of a multiple charged relativistic heavy ion (RHI) its velocity decreases during penetration through a radiator due to the ionization energy loss. Accordingly, calculations of VChR characteristics from RHI (more precisely, optical mixed Cherenkov-Bremsstrahlung radiation) become more complex — see [8–11] and references therein — it is necessary to apply numerical methods of calculation to take the most accurate account of RHI slowing-down. A noticeable broadening of the VChR angular distribution should be taken into account when calculating the efficiency of Cherenkov detectors [12], especially at energies of 100–300 MeV/u (near the maximum of ionization losses) [12, 13].

However, some of the characteristics of the VChR from RHI, taking into account the slowing-down in a thin radiator are possible to analyse qualitatively and even quantitatively, using the analogy with the Fresnel diffraction theory. This is the purpose of the work.

2 The Cornu spiral and its relevance to VChR theory

Let us start with the well-known formula [14] to calculate the spectral-angular distributions of the radiation intensity from RHI moving in a radiator in an arbitrary trajectory $r(t)$:

$$\frac{dW}{d\omega d\Omega} = \frac{(Ze)^2\,\omega^2}{4\pi^2 c^3}\sqrt{\varepsilon(\omega)}\left|\int_0^T [\mathbf{n}\times[\mathbf{n}\times\mathbf{v}(t)]]\exp\left[i\omega\left(t-\sqrt{\varepsilon(\omega)}\frac{\mathbf{n}\cdot\mathbf{r}(t)}{c}\right)\right]dt\right|^2, \tag{2.1}$$

where $\mathbf{n} = \{\sin\theta\cos\varphi, \sin\theta\sin\varphi, \cos\theta\}$ — is the unit vector defining the direction of radiation, c — is the speed of light in a vacuum; Ze — is the RHI charge; $\sqrt{\varepsilon(\omega)}$ — is the radiator refractive index at the frequency ω; $\mathbf{v}(t)$ — is the RHI velocity in a radiator; T — is its time of flight through a radiator; λ and $\omega = 2\pi c/\lambda$ — are the radiation wave length and frequency, respectively.

Let the RHI be moving in the radiator in a rectilinear trajectory along the selected Z axis, directed along its velocity $\mathbf{v}(t)$, then eq. (2.1) converts to:

$$\frac{dW}{d\omega d\Omega} = \frac{(Ze\sin\theta)^2\,\omega^2}{4\pi^2 c^3}\sqrt{\varepsilon(\omega)}\left|\int_0^L \exp\left[i\omega\left(t(z)-\sqrt{\varepsilon(\omega)}\frac{z\cos\theta}{c}\right)\right]dz\right|^2, \tag{2.2a}$$

where L — is the radiator thickness. The transition from the time integral to the path integral is performed in the following way: $v(t)dt = dz$, $t(z) = \int_0^z d\xi/v(\xi)$.

The integral in eq. (2.2a) actually defines the formation path of radiation [1, 7]:

$$\int_0^L \exp\left[i\omega\left(t(z)-\sqrt{\varepsilon(\omega)}\frac{z\cos\theta}{c}\right)\right]dz \tag{2.2b}$$

If we assume that the RHI velocity in a radiator does not change — ($v(t) = v_0$, $\beta_0 = v_0/c$, $t(z) = z/v_0$), i.e. we neglect the RHI energy loss (slowing-down), the integral (2.2b) transforms to:

$$\int_0^L \exp\left[i\omega\left(\frac{z}{v_0}-\sqrt{\varepsilon(\omega)}\frac{z\cos\theta}{c}\right)\right]dz = \int_0^L \exp\left[i\omega\frac{z}{v_0}\left(1-\sqrt{\varepsilon(\omega)}\beta_0\cos\theta\right)\right]dz \tag{2.3}$$

The integrals in eqs. (2.1)–(2.3) are similar to the integrals arising in the theory of light diffraction, see, e.g. [15]. The integral (2.3) is actually the Huygens principle, according to which the waves are summing up from the entire trajectory of the length L, which here plays the role of a "gap" from the diffraction theory point of view. I.M. Frank first applied this principle to get the simple physical explanation of the VChR origin. The latter occurs when the radiation formation path (2.3) is maximal, i.e. when the emitted waves are summing up in the phase, which occurs at the Cherenkov angle:

$$\cos\theta_{C0} = 1/\beta_0\sqrt{\varepsilon(\omega)} \tag{2.4}$$

Thus, the eq. (2.2a) for the spectral-angular distribution of the (VChR) radiation intensity in the case of constant RHI velocity $v(t) = v_0$ has the form:

$$\frac{dW}{d\omega d\Omega} = \frac{(Ze\sin\theta)^2\,\omega^2\sqrt{\varepsilon(\omega)}}{4\pi^2 c}\beta_0^2\left|\int_0^T \exp\left[i\omega t\left(1-\sqrt{\varepsilon(\omega)}\beta_0\cos\theta\right)\right]dt\right|^2 \tag{2.5}$$

The angular distribution of VChR from RHI calculated using eq. (2.5) is a narrow peak with a maximum at the radiation angleθ equal to the Cherenkov angle θ_{C0} (2.4) and half-width (FWHM) $\Delta\theta_{TF} = \lambda/L\sqrt{\varepsilon(\omega)}$ (see in [16]).

Further, let us consider RHI moving in a radiator in a rectilinear trajectory but with a velocity permanently decreasing due to the ionization energy losses. For a thin radiator [8–11], the RHI velocity at the exit of the radiator of thickness L is approximately:

$$1/v_L \cong 1/v_0 - L\zeta/v_0^2, \tag{2.6}$$

where v_0, v_L — are the initial and the final RHI velocities, $\zeta = -c^2 S(E_0)/\gamma_0^3 v_0 M c^2$, $S(E_0) = -dE/dz|_{z=0}$ — is the radiator stopping power, E_0 — is the RHI initial energy.

Now the integral (2.2b) takes the form:

$$\begin{aligned} I &= \int_0^L \exp\left[i\omega\left(z\left(\frac{1}{v_0} - \sqrt{\varepsilon(\omega)}\frac{\cos\theta}{c}\right) - z^2\left(\frac{\zeta}{2v_0^2}\right)\right)\right] dz = \\ &= \int_0^L \exp\left[i\omega\left(z\left(\frac{1}{v_0} - \sqrt{\varepsilon(\omega)}\frac{\cos\theta}{c}\right)\right)\right] \cdot \exp\left(-z^2\left(\frac{\zeta}{2v_0^2}\right)\right) dz \end{aligned} \tag{2.7}$$

In this form, the eq. (2.7) actually corresponds to the mathematical formulation of the Huygens-Fresnel principle (see, e,g, [15]): the light field at the point P is the result of the superposition of light waves emitted by the surface (Σ) elements ($d\sigma$):

$$E(P) = \int_\Sigma E(M) \cdot \frac{\exp(-ik\rho)}{\rho} \cdot K(\phi) \cdot d\sigma, \tag{2.8}$$

where $E(P)$, $E(M)$ — are the complex amplitudes of the filed at the points P and M, $k = \omega/c = 2\pi/\lambda$ — is the wavenumber of the light wave, $K(\phi)$ — is the so-called slope coefficient, which takes into account the fact that the element's $d\sigma$ contribution to the resultant field depends on the orientation of this surface element with respect to the observation point.

Comparing (2.8) and (2.7), we see that the second exponential in eq. (2.7) plays the role of the slope coefficient, related to the slowing-down of RHI in the radiator (the analogy with the slope coefficient is straight: if the velocity decreases, the radiation *angle* changes).

The process of the VChR formation from RHI in the radiator looks as follows: during the motion in the radiator, the RHI polarizes the radiator atoms. According to the Huygens-Fresnel principle, each point on the RHI path becomes a source of spherical waves. Taking into account the slowing-down, there appear to be additional (compared to penetration with constant velocity) phase shifts of emitted waves. The detector records the result of the interference of these waves emitted from all parts of the RHI trajectory.

In the case of a thin radiator, the integral of the eq. (2.7) can be calculated and we arrive at the following expression for the VChR from RHI taking account of slowing-down:

$$\frac{dW}{d\omega d(\cos\theta)} = \omega L\left(\frac{Ze\sin\theta}{c}\right)^2 f(\theta,\omega), \tag{2.9a}$$

$$f(\theta,\omega) = \frac{1}{2\Delta\theta_s \sin\theta_{C0}}\left((C(u_L) - C(u_0))^2 + (S(u_L) - S(u_0))^2\right) \tag{2.9b}$$

$$u_0 = \sqrt{\frac{\omega}{\pi|\zeta|}}\left(1 - \sqrt{\varepsilon(\omega)}\beta_0\cos\theta\right), \qquad \zeta = -c^2 S(E_0)/\gamma_0^3 v_0 M c^2, \tag{2.10}$$

$$u_L = u_0 + \sqrt{\frac{\omega|\zeta|}{\pi}}\frac{L}{v_0} = u_0 + \sqrt{\frac{\omega|S(E_0)|c^2}{\pi\gamma_0^3 v_0^3 M c^2}} \cdot L. \tag{2.11}$$

In eq. (2.9b), the $\Delta\theta_s$ determines the width of the angular distribution of the VChR from RHI, which linearly depends on the thickness L of the radiator, reflecting the slowing-down [8]:

$$\Delta\theta_s = \theta_{C0} - \theta_{CL} = \frac{1}{\gamma_0^3 \beta_0^2 M c^2} \frac{1}{\sqrt{\left(\beta_0 \sqrt{\varepsilon(\omega)}\right)^2 - 1}} S(E_0) L, \tag{2.12}$$

where θ_{C0} and θ_{CL} — are VChR angles at the RHI entrance and exit of the radiator of thickness L calculated using the eq. (2.4) with RHI velocities v_0 and v_L correspondingly (the index s means here «stopping»).

In the eq. (2.9b) $C(u) = \int_0^u \cos\left[\frac{\pi}{2}t^2\right] dt$, $S(u) = \int_0^u \sin\left[\frac{\pi}{2}t^2\right] dt$ — are the Fresnel integrals. The argument u_0 (2.10) depends on the angle and frequency of the radiation and on the refractive index $\sqrt{\varepsilon(\omega)}$, while u_L (2.11) depends on the stopping power $S(E_0) = -dE/dz|_{z=0}$ and thickness L of the radiator as well.

In the diffraction theory of light, the expression, entering the eq. (2.9b),

$$\xi^2(u_0, u_L) = \left((C(u_L) - C(u_0))^2 + (S(u_L) - S(u_0))^2\right), \tag{2.13}$$

is the squared length between two points of the "Cornu spiral" (clothoid). The Cornu's spiral — is a graphical method for constructing diffraction patterns — e.g. at edge diffraction or at slit diffraction [15]. The formulae describing these diffractive patterns just contain the expressions similar to the eq. (2.13). When drawing the Cornu spiral on the (x, y) plane, the Cartesian coordinates equal to the values of the Fresnel integrals, i.e. $x = C(u)$, $y = S(u)$. With a continuous change in the parameter u, these points form a smooth curve — the Cornu spiral.

Thus, the formula for the spectral-angular distributions of VChR from RHI now reads:

$$\frac{dW}{d\omega d(\cos\theta)} = \omega L \left(\frac{Ze}{c}\right)^2 \frac{\sin^2\theta}{2\Delta\theta_s \sin\theta_{C0}} \xi^2(u_0, u_L). \tag{2.14}$$

The square of the length of the segment between points of the Cornu spiral $(x_0, y_0) = (C(u_0), S(u_0))$, $(x_L, y_L) = (C(u_L), S(u_L))$, multiplied by $\sin^2\theta$, determines the shape of the VChR angular distribution intensity. The arguments u_0 and u_L of the Fresnel integrals for the selected radiation angle are calculated using the eqs. (2.10)–(2.11).

Thus, the eqs. (2.9)–(2.12) for calculating the spectral-angular distributions of VChR from RHI in a thin radiator taking account of slowing-down contain the Fresnel integrals and predict the appearance of a complex diffraction-like structure of both spectral and angular distributions of VChR from RHI — see [8–11, 16] and references therein.

We would like to stress here, if one takes account of RHI slowing-down, one deals with the *mixed* Cherenkov-Bremsstrahlung radiation. This radiation resembles the Synchrotron-Cherenkov radiation of high-energy cosmic particles in the Earth's atmosphere, when the trajectory is curved by the Earth's magnetic field and simultaneously the medium acts. The details on Synchrotron-Cherenkov radiation and similar effects (not relating to RHI radiation) can be found in [2]. In our case, the RHI trajectory remains rectilinear but the deceleration appears and the radiation process is going on again in the medium.

During the RHI penetration through a radiator, the transition radiation also occurs [11], however it is generated only at radiator boundaries, and its intensity in the optical region is much less than the mixed optical Cherenkov-Bremsstrahlung, which is formed throughout the entire RHI trajectory in the radiator [1, 2].

3 Angular distributions of VChR from RHI — interpretation using the Cornu spiral

To proceed with the further analysis using the Cornu spiral let us first demonstrate the angular distributions of VChR (see in figure 1) calculated for different radiator thicknesses using the eqs. (2.9)–(2.11).

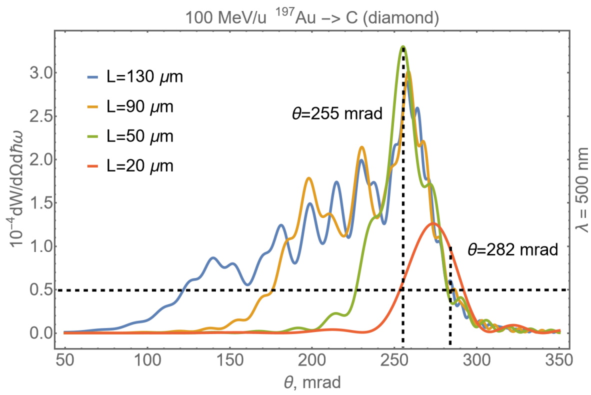

Figure 1. The angular distributions of VChR from 100 MeV/u Au RHI in a diamond radiator of thickness $L = 20$, $L = 50$ and $L = 90\,\mu$m (corresponding numbers near each curve). The slowing-down $S(E_0) = -14264.7[\mathrm{keV}/\mu\mathrm{m}]$ is calculated according to the Bethe-Bloch formula [12, 13], $\lambda = 500$ nm and $\sqrt{\varepsilon} = 2.43$. The vertical lines correspond to the emission angles $\theta_{C0} = 282$ mrad (initial Cherenkov angle) and $\theta = 255$ mrad (position of maximal on the curve for $L = 50\,\mu$m), the horizontal line corresponds to intensity level = 5000.

Looking at figure 1, one can make the following conclusions on VChR angular distributions changes caused by an increase of the radiator thickness:

- At the initial Cherenkov cone ($\theta = \theta_{C0}$), with increasing the radiator thickness from 20 to 50 and up to 90 microns, the radiation intensity decreases more than two times.
- The radiation escapes from the initial Cherenkov cone towards smaller emission angles. Qualitatively, this predicts the eq. (2.4), but an accurate calculation gives a more interesting picture of the escape, showing the formation of a diffraction-like structure of the angular distribution and the growth of its localization area. For example, at $dW/d\omega d(\cos\theta) = 5000$ (the horizontal line in figure 1), the latter grows from about 35 mrad ($L = 20\,\mu$m) to 60 mrad ($L = 50\,\mu$m) and up to 125 mrad ($L = 90\,\mu$m).

We suggest the following way to make a qualitative analysis of the appearance and change of diffraction-like VChR angular distribution from RHI, with L increase. a) Take the (universal) Cornu spiral plot (see, for example, [17]); b) Calculate the necessary Fresnel integrals for the selected emission angle θ — eqs. (2.10)–(2.11) and define coordinates $x_1 = C(u_0)$, $y_1 = S(u_0)$ and $x_2 = C(u_L)$, $y_2 = S(u_L)$; c) Put two points onto the Cornu spiral plot, measure the distance between them and calculate the ratio of the squares of the distances.

Let us demonstrate this method to explain some features of the graphs presented in figure 1: how the VChR intensity changes at a fixed emission angle θ with a change in the thickness of the radiator. The necessary numbers are given in the table 1.

In figure 2a, the end of the arrow emerging from zero, with an increase in the thickness L from 20 to 50 and further up to 90 microns makes the journey (is twisting) along a spiral, while the length of the arrow changes, reflecting the decrease in the emission intensity at the initial Cherenkov angle, i.e. at $\theta = \theta_{C0}$.

As we mentioned above, the Cornu spiral plot is universal, but to demonstrate how it looks like in relation to our investigations, figure 2b shows the Cornu spiral as a function of the u_0 argument. The θ parameter changes from 50 µm to 350 µm (the same range as in figure 1).

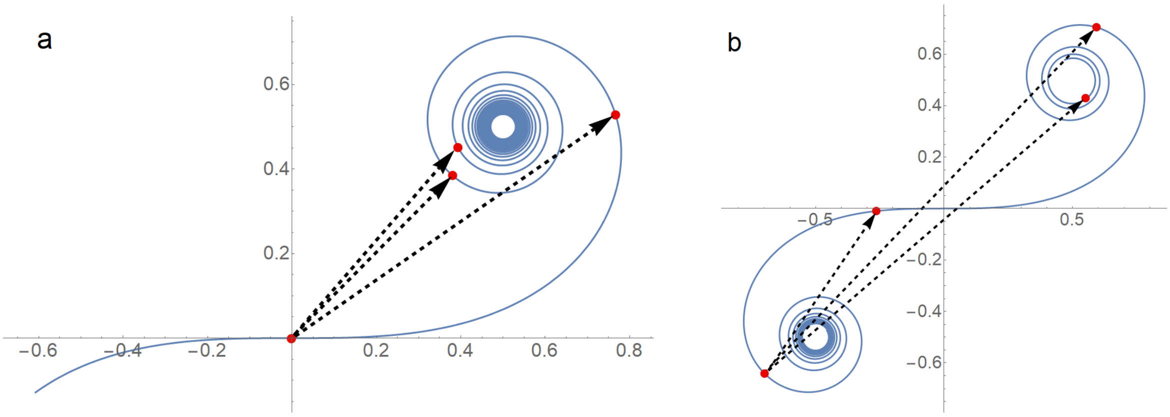

Figure 2. Journey along the Cornu spiral: variations in the length of the distance ξ with increasing radiator thickness (indicated for L = 20, 50 and 90 microns), illustrating the change in the intensity of the VChR angular distribution at the initial Cherenkov cone $\theta = \theta_{C0}$ = 282 mrad (a) and at θ = 255 mrad (b) (corresponds to the maximum in figure 1).

In figure 2b, arrows make a similar journey, leaving the starting point on the spiral corresponding to θ = 255 mrad. In this case, the variation in the length of the arrow is much stronger, which reflects the formation and weakening of the “diffraction” maximum — in accordance with figure 1.

The relative change in the intensity characterizes the last column of table 1. Formally, a further increase in the thickness of the radiator will correspond to an approach of the arrow end to the Cornu spiral focus, thus to the asymptotic value of the length of the arrow. However, one should be careful here since the developed theory is valid only if the expansion eq. (2.6) limiting the maximum values of L is valid.

Table 1. Calculated numbers of Fresnel arguments u_0, u_L and integrals $C(u_0)$, $C(u_L)$, $S(u_0)$, $S(u_L)$ for two VChR emission angles and three radiator thicknesses. The last column contains the ratio of squared distances between two points of the Cornu spiral plot.

L, µm	u_0	u_L	$C(u_0)$	$C(u_L)$	$S(u_0)$	$S(u_L)$	$\frac{\xi^2(u_0,u_{L=20})}{\xi^2(u_0,u_L)}$
Angle θ = 255 mrad							
20	−1.334	−0.25	−0.6	−0.25	−0.7	−0.008	1
50	−1.334	1.35	−0.6	0.58	−0.7	0.7	5.58
90	−1.334	3.51	−0.6	0.54	−0.7	0.42	4.25
Angle $\theta = \theta_{C0}$ = 282 mrad							
20	0	1.07	0	0.77	0	0.51	1
50	0	2.69	0	0.38	0	0.45	0.4
90	0	4.84	0	0.45	0	0.45	0.47

2024 JINST 19 C11011

Similarly, one can interpret a diffraction-like angular distribution arising at the fixed thickness of the radiator. In this case, both arguments of the Fresnel integrals (u_0, u_L) depend on the angle θ and the spiral journey looks more complicated.

The figure 3 shows the results of the evolution of the Cornu spiral as a function of the radiator thickness. The ion and target parameters are the same as in figure 1. It can be seen that as the length of the radiator increases, the Cornu spiral redistributes to the first quarter. The situation in figure 3d corresponds to the limit value of the radiator thickness $L \approx 124\,\mu\text{m}$. It arises due to the fact that when RHI moves in a radiator with a decreasing velocity after a certain thickness the condition for the occurrence of VChR is violated.

2024 JINST 19 C11011

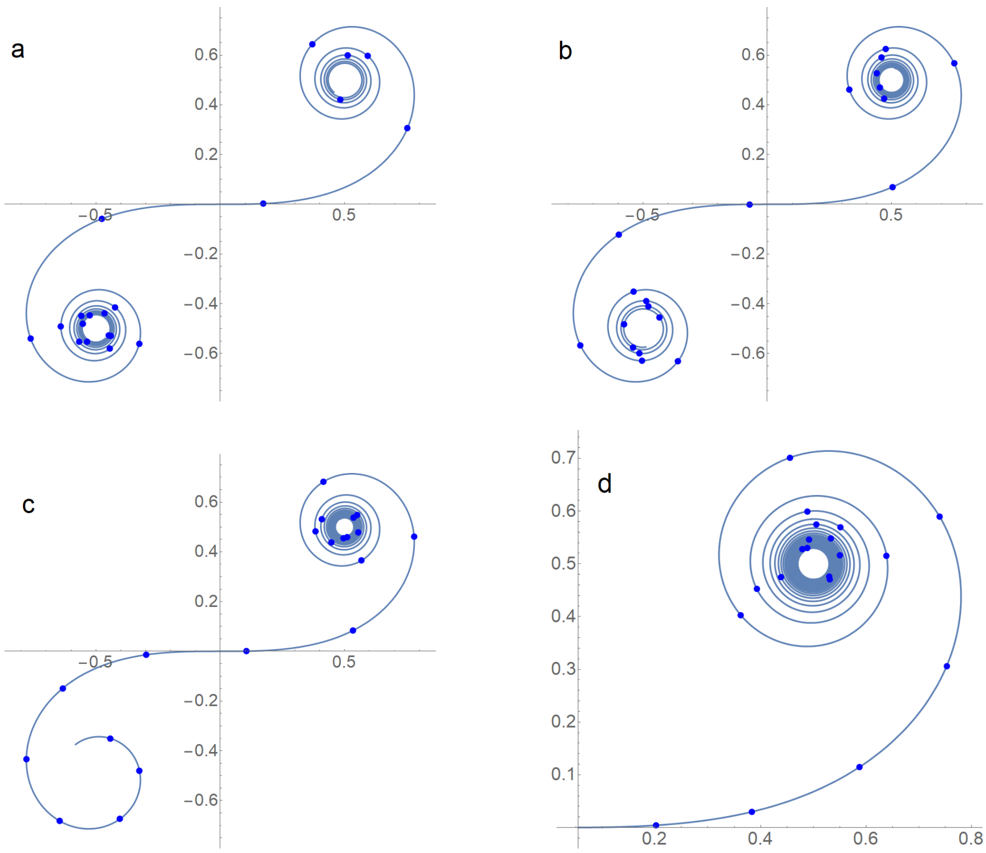

Figure 3. Dynamics of the Cornu spiral as a function of the u_L argument with increasing target thickness: $L = 20\,\mu\text{m}$ (a), $L = 50\,\mu\text{m}$ (b), $L = 90\,\mu\text{m}$ (c) and $L = 130\,\mu\text{m}$ (d). The dots show the 20 mesh levels evenly spaced in the θ parameter directions from 50 µm to 350 µm.

Let us explain the possible application of the above investigations to the estimation of the VChR angular distribution width. It can be seen that the Cornu spiral as a function of the u0 argument starts in the third quarter and as the θ parameter changes from 50 µm to 350 µm it transits to the first quarter (figure 2b). On figure 3d for the 130 µm target the Cornu spiral as a function of the u_L argument starts and ends in the first quarter. So for a wide range of the θ parameter values the distance between points on the Cornu spiral $x_1 = C(u_0)$, $y_1 = S(u_0)$ and $x_2 = C(u_L)$, $y_2 = S(u_L)$ will be significant. Figure 1 shows that the widest VChR range is exactly for the 130 µm target.

4 Conclusion

The connection of the theory of VChR from RHI taking account of slowing-down in a thin radiator to the Fresnel diffraction theory is considered. We showed how the Cornu spiral arises in this theory and is useful to qualitatively analyse the shape and quickly estimate the width of the angular distribution of VChR from RHI. However this needs a more detailed revision and further investigations will be published later. For the thicker radiators, it is necessary to integrate numerically eq. (2.2a) using the software packages (SRIM, ATIMA), which more correctly compare to the Bethe-Bloch formula describing the slowing-down of RHI in a radiator. This method was recently applied to take account of RHI slowing-down in a thick liquid Cherenkov radiator — a prototype of RHI TOF detector.

To conclude: a significant broadening of the VChR angular distribution caused by RHI energy loss (slowing-down) in a solid radiator should be taken into account in estimations of the efficiency of Cherenkov detectors, especially at energies of 100–300 MeV/u (near the maximum of ionization losses) [3] and when the refraction or total internal reflection of optical radiation (for example, DIRC [12]) is important.

We note also other interesting new findings in theory [6, 18, 19] and possible applications of the RHI Cherenkov radiation: the velocity filter and even the charge-mass filter [20] of relativistic fragments.

The experiments devoted to the study of the described properties of VChR from RHI are included in the Super-FRS collaboration programme at the FAIR (Darmstadt) accelerator complex [21] and the authors hope for experimental confirmation of the predicted effects in the near future.

Acknowledgments

The authors are grateful to Yu. Pivovarov, H. Geissel and C. Scheidenberger for numerous useful discussions. The research was carried out with the support of a grant from the Government of the Russian Federation (Agreement No. 075-15-2024-667 of 23 August 2024).

References

[1] I.M. Frank, *Vavilov-Cherenkov radiation*, Nauka, Moscow (1988).

[2] G.N. Afanasiev, *Vavilov-Cherenkov and Synchrotron Radiation: Foundations and Applications*, Springer (2004) [DOI:10.1007/1-4020-2411-8].

[3] N. Kuzminchuk-Feuerstein et al., *Time-of-Flight measurements with a detector using a liquid Cherenkov radiator-prototype of a possible TOF detector for the Super-FRS at FAIR*, Nucl. Instrum. Meth. A **923** (2019) 34.

[4] O.V. Bogdanov, P.O. Kazinski and G.Y. Lazarenko, *Proposal for experimental observation of the twisted photons in transition and Vavilov-Cherenkov radiations*, 2020 *JINST* **15** C04052 [arXiv:2001.05229].

[5] V.M. Grichine, *Radiation of arbitrary moving charge in an absorbing medium*, *Radiat. Phys. Chem.* **67** (2003) 93.

[6] C. Roques-Carmes et al., *Nonperturbative Quantum Electrodynamics in the Cherenkov Effect*, *Phys. Rev. X* **8** (2018) 041013.

[7] B.M. Bolotovskii, *Vavilov-Cherenkov radiation: its discovery and application*, *Phys. Usp.* **52** (2009) 1099.

[8] E.S. Kuzmin and A.V. Tarasov, *Diffractionlike effects in angular istribution of Cherenkov radiation from heavy ions*, *JINR Rapid Commun.* **4[61]-93** (1993) 64.

[9] E.I. Rozhkova and Y.L. Pivovarov, *Mixed optical Cherenkov-Bremsstrahlung radiation in vicinity of the Cherenkov cone from relativistic heavy ions: Unusual dependence of the angular distribution width on the radiator thickness*, *Phys. Lett. A* **380** (2016) 2386.

[10] O.V. Bogdanov, E.I. Fiks and Y.L. Pivovarov, *Optical radiation from channeled relativistic heavy ions in vicinity of the Cherenkov angle*, *Nucl. Instrum. Meth. B* **355** (2015) 86.

[11] E.I. Fiks and Y.L. Pivovarov, *Interference effects in angular and spectral distributions of X-ray Transition Radiation from Relativistic Heavy Ions crossing a radiator: Influence of absorption and slowing-down*, *Nucl. Instrum. Meth. B* **355** (2015) 184.

[12] C. Grupen and B. Shwartz, *Particle Detectors*, Cambridge Monographs on Particle Physics, Nuclear Physics and Cosmology, 2nd Edition, Cambridge University Press (2008) [DOI:10.1017/CBO9780511534966].

[13] P. Sigmund, *Particle Penetration and Radiation Effects Volume 2: Penetration of Atomic and Molecular Ions*, Springer (2014) [DOI:10.1007/978-3-319-05564-0].

[14] J.D. Jackson, *Classical Electrodynamics*, 3rd Edition, John Wiley and Sons (1998).

[15] M. Born and E. Wolf, *Principles of Optics: Electromagnetic Theory of Propagation, Interference and Diffraction of Light*, 7th Edition, Cambridge University Press (1999) [DOI:10.1017/CBO9781139644181].

[16] E.I. Fiks et al., *Influence of slowing down in the radiator on the Cherenkov radiation angular distributions from relativistic heavy ions at FAIR, SPS and LHC energies*, *Nucl. Instrum. Meth. B* **309** (2013) 146.

[17] M. Abramowitz and I.A. Stegun, *Handbook of Mathematical Functions*, National Bureau of Standards (1972).

[18] T. Yamaguchi et al., *Cherenkov light detection as a velocity selector for uranium fission products at intermediate energies*, *Nucl. Instrum. Meth. A* **766** (2014) 123.

[19] V.S. Malyshevsky, G.V. Fomin and I.A. Ivanova, *Modeling the detector of charge states of relativistic multicharged ions*, *Tech. Phys. Lett.* **43** (2017) 71.

[20] O.V. Bogdanov, E.I. Rozhkova, Y.L. Pivovarov and N. Kuzminchuk-Feuerstein, *Mass dependence of spectral and angular distributions of Cherenkov radiation from relativistic isotopes in solid radiators and its possible application as mass selector*, 2018 *JINST* **13** C02015.

[21] I. Tanihata et al., *Conceptual Design Report for the Scientific Program of the Super-FRS Experiment Collaboration*, GSI Report 2016-3 (2016) [DOI:10.15120/GSI-2016-03763].

2024 JINST 19 C11011